Low-energy collective dynamics of charge stripes in the doped nickelate $La_{2-x}Sr_xNiO_{4+\delta}$ observed with optical conductivity measurements

J. Lloyd-Hughes,[1,*] D. Prabhakaran,[1] A. T. Boothroyd,[1] and M. B. Johnston[1,†]
[1]*Department of Physics, Clarendon Laboratory, University of Oxford, Parks Road, Oxford OX1 3PU, United Kingdom*
(Received 26 February 2008; published 14 May 2008)

We have investigated charge dynamics in the static stripe ordered phase of $La_{2-x}Sr_xNiO_{4+\delta}$ at lattice temperatures below the charge ordering transition, via optical conductivity measurements at low energies (1–10 meV). The thermally activated dynamic response of the charge stripes is found to be characteristic of a collective mode such as a pinned charge density wave. At incommensurate doping levels, the pinning energy is reduced, owing to the presence of real-space defects in the stripe order, and a pronounced increase in the oscillator strength is seen. The results provide compelling evidence for the existence of low-energy collective modes of the charge stripes.

DOI: 10.1103/PhysRevB.77.195114 PACS number(s): 71.45.Lr, 73.20.Mf, 75.30.Fv

The ordering of both charges and spins into striped phases in doped nickelates and cuprates has been the subject of intense recent research, owing to possible links with high-T_c superconductivity.[1,2] While static stripe phases are thought to limit electron motion and thus hinder superconductivity, dynamic stripe correlations[3] could be present and play an important role in high-T_c materials.[4,5] Collective *spin dynamics* of these systems have been observed with characteristic energies in the meV range.[6,7] However, to date, there have been no measurements of collective *charge dynamics* in this energy range.

Evidence for the ordering of charges and spins in the layered nickelate $La_{2-x}Sr_xNiO_{4+\delta}$ (LSNO) into stripes has been provided by electron,[8] neutron,[9,10] and x-ray[11] scattering. Macroscopic properties such as the specific heat capacity, magnetization, and dc resistivity are also dramatically changed by stripe formation.[12–14] In addition, the optical conductivity exhibits a pseudogap with an energy 2Δ in the midinfrared[15] that opens below the charge stripe ordering temperature, and which is most pronounced at low temperatures. For Sr doping, this behavior has been observed for commensurate[14,15] and incommensurate[16] charge stripes, with $2\Delta=0.25$ eV and $2\Delta\sim0.1$ eV, respectively. A pseudogap has additionally been observed for O doping,[15,17] with $2\Delta\sim0.1$ eV. The underlying mechanism of pseudogap formation remains contentious, however, being alternatively assigned to charge density wave (CDW) formation[14] or to a single-particle (polaronic) transition in the midinfrared with a Drude response at lower frequencies.[15,17] The Drude model predicts a peak in the conductivity at zero frequency, and is valid for a noninteracting gas of delocalized charges.

The optical conductivity of a CDW, a quasi-one-dimensional modulation of charge density, is dramatically different from that of the Drude model. A broad single-particle response exists above an energy gap 2Δ (created by the Peierls transition), while a lower-energy collective mode resides within the gap.[18] Defect sites pin the phase of the CDW, resulting in the collective mode having a peak conductivity at a finite energy $\hbar\omega_0$ substantially below 2Δ (for weak pinning). Typically, ω_0 is in the gigahertz to terahertz frequency range.[18] Evidence for CDWs has been reported in a variety of materials, including manganites[19] and cuprates.[20]

Terahertz time-domain spectroscopy provides a direct probe of the complex conductive response of a material[21–23] and hence may be used to observe low-energy charge correlations. Specifically, the form of the frequency dependent conductivity of a material such as LSNO provides evidence about the existence and origin of charge correlation. We have measured the complex conductive response of charge stripes in LSNO over the terahertz frequency range, using time-domain spectroscopy. We find that the charge stripes exhibit a collective mode consistent with pinned charge density waves, rather than a delocalized (Drude-like) response.

The charge stripe ordering in the *ab* plane of LSNO is schematically illustrated in Fig. 1. When $x=0.333$, the charge stripes (shaded regions, representing high charge density) are commensurate with the square lattice of Ni sites, with period 3 in the *a* and *b* directions. Charge ordering is partly stabilized by regions of antiferromagnetic order between the stripes. In contrast, at an incommensurate doping such as $x=0.275$, the charge stripes can be spaced with period 3 or 4, as transmission electron micrographs indicate.[24] This can create kinks in the stripe, and larger interstripe gaps, respectively labeled A and B in Fig. 1. Increasing the lattice temperature is expected to enhance the density of these defects for both incommensurate and commensurate dopings, until static charge stripe order is destroyed above T_{co}. Charge

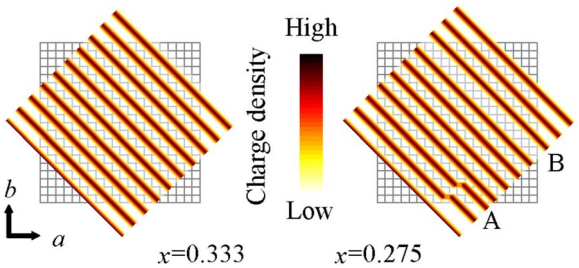

FIG. 1. (Color online) Charge stripe structure in *ab* plane of LSNO. At a commensurate doping level $x=0.333$, the charge stripes (colored bands) diagonally run across the NiO_2 lattice (solid lines), and are separated by antiferromagnetic regions (light areas). With an incommensurate doping such as $x=0.275$, kinks in the stripes can appear (A), and there can be regions with larger interchain spacing (B).

 ©2008 The American Physical Society

stripe ordering is correlated over distances of ~70 unit cells for $x=0.333$, and ~40 unit cells for $x=0.275$.[25] On larger length scales, there is no preference for either diagonal of the square lattice, and macroscopic measurements therefore yield properties averaged over the *ab* plane.

Here, we report on terahertz conductivity measurements of commensurate ($x=0.333$) and incommensurate ($x=0.275$) nickelate crystals. We chose to compare these compositions as the presence of defects in the charge stripes of an incommensurate sample would necessarily correspond to a modification of the collective dynamics relative to a commensurate one, and thus would be one indication of the presence of collective modes.

High quality single crystals of $La_{2-x}Sr_xNiO_{4+\delta}$ with $x=0.333$ and $x=0.275$ were grown by the floating-zone method.[26] The oxygen doping level was determined to be $\delta=0.01-0.02$ for both crystals by thermogravimetric analysis.[13] Samples were cut, polished, and thinned in the *c* direction before mounting in the variable-temperature insert of a cryostat. The transmission of single-cycle pulses of terahertz radiation (polarized in the *ab* plane) through the sample was measured in a terahertz time-domain spectroscopy setup similar to that described in Ref. 27. The time-domain measurement allowed the complex conductivity to be determined without use of the Kramers–Kronig relations, and with a high signal-to-noise ratio in comparison to incoherent techniques such as Fourier transform infrared spectroscopy. By comparison to the reference pulse, the *ab* plane complex dielectric function $\epsilon(\omega)$ was determined[27] over the frequency range 0.2–2.4 THz (1–10 meV) at various sample temperatures. The complex conductivity σ was then calculated from $\sigma(\omega)=(\epsilon(\omega)-\epsilon_1)\omega\epsilon_0/i$ where $\epsilon_1=81$ is the dielectric constant above the lowest TO phonon mode. Here, ϵ_1 was calculated from the oscillator strength of the lowest TO mode[16] and the value of the measured real dielectric constant at low frequency ($\epsilon_s=106$).

The complex conductivity σ of the commensurate charge stripe system ($x=0.333$) is now discussed with reference to Fig. 2. At a lattice temperature of 1.5 K, the real part of the conductivity Re[σ] is minimal in the range 0–6 meV, while the imaginary part Im[σ] is large, negative, and dispersive. The dashed lines in Figs. 2(a) and 2(b) show the conductivity of the 19 meV TO-phonon mode using the Drude–Lorentz model with the parameters of Ref. 16. A low-frequency shoulder to the phonon mode[16] explains the discrepancy between the modeled and measured Re[σ].

As the lattice temperature T is increased, Re[σ] begins to increase dramatically below 6 meV, as evidenced by the data above $T=70$ K. The observed rise in Re[σ] with photon energy at all temperatures is inconsistent with the Drude response of free charges, which predicts that Re[σ] is peaked at zero frequency. In contrast to Re[σ], Im[σ] is almost invariant with temperature [Fig. 2(b)].

In Fig. 3(a), Re[$\sigma(E)$] is plotted in the range $T=1.5-230$ K. In the region defined by $T<120$ K, $E<6$ meV, the conductivity is minimal. However, close to $T_{co}=240$ K, the conductivity at low energies (2–6 meV) rapidly increases. This correlation with T_{co} is illustrated by Re[σ] at 5 meV in Fig. 3(b) (crosses), which diverges close to $T_{co}=240$ K.[9]

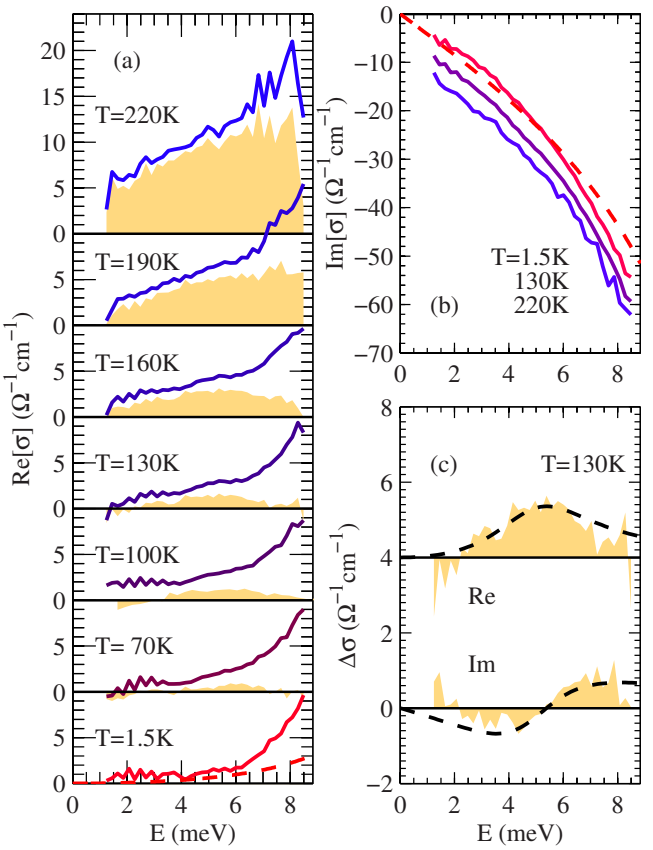

FIG. 2. (Color online) Low-energy conductivity σ of commensurate LSNO ($x=0.333$). (a) Re[σ] (solid lines) is minimal below 6 meV at low temperature, and increases at higher temperatures. (b) Im[σ] (solid lines, offset vertically for clarity by $-5\ \Omega^{-1}\,\mathrm{cm}^{-1}$ for $T=130$ K and $-10\ \Omega^{-1}\,\mathrm{cm}^{-1}$ for $T=220$ K) is not strongly temperature dependent. The dashed lines in (a) and (b) show the modeled σ of the lowest TO-phonon mode (see text). The shaded areas in (a) and (c) show $\Delta\sigma=\sigma(T)-\sigma(T=1.5\ \mathrm{K})$, and demonstrate the presence of pinned charge density waves with a conductivity σ_{CDW} [Eq. (1)] shown by the dashed lines in (c).

We identify the origin of the stripe conductivity at elevated temperatures by defining the thermally induced conductivity change $\Delta\sigma(T)=\sigma(T)-\sigma(T=1.5\ \mathrm{K})$. In Fig. 2(a), the shaded areas show the real part of $\Delta\sigma(T)$. A peak in Re[$\Delta\sigma$] around 5 meV has a complementary zero crossing in Im[$\Delta\sigma$], as can be seen in Fig. 2(c). An excellent agreement with experiment was obtained using

$$\sigma_{CDW}(\omega)=\frac{\sigma_0\Gamma}{i}\frac{\omega}{\omega_0^2-\omega^2-i\omega\Gamma} \qquad (1)$$

as the dashed lines in Fig. 2(c) indicate. This functional form is that of a CDW pinned by lattice defects[18] with a pinning energy $\hbar\omega_0$. In this expression, the oscillator strength is $\sigma_0\Gamma=ne^2/m^*$, where n is the charge density, e is the electron charge, and m^* is the carrier effective mass. Γ is the damping rate of the oscillation. The values obtained from the fit were $\sigma_0=1.3\ \Omega^{-1}\,\mathrm{cm}^{-1}$, $\Gamma=7\times10^{12}\ \mathrm{s}^{-1}$, and $\hbar\omega_0=5.4$ meV. CDWs have been reported in the manganites[19] with comparable pinning energies and damping rates. In our case, the

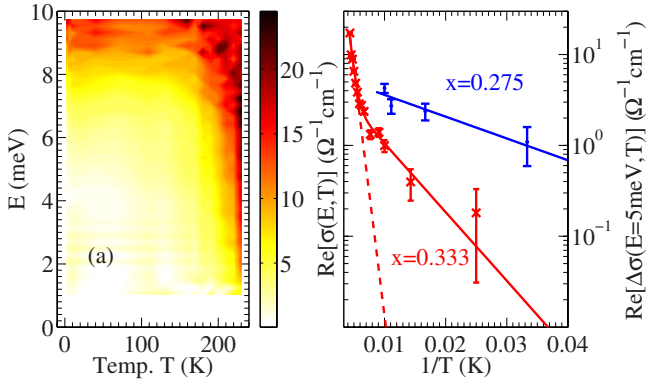

FIG. 3. (Color online) Evolution of the conductivity with temperature. (a) The real part of the conductivity for $x=0.333$ at temperatures 1.5 K-230 K. (b) Re$[\Delta\sigma]$ at $E=5$ meV (crosses) can be seen to rapidly increase as the charge ordering temperature $T_{co}=240$ K is approached. The dashed line is a fit to the temperature dependence of Re$[\Delta\sigma]$ at high temperature using Eq. (2), while the solid line has two such terms, as described in the text. For $x=0.275$, Re$[\Delta\sigma(E=5\text{ meV},T)]$ (points) is substantially higher than that for $x=0.333$, and $E_a=4.8$ meV.

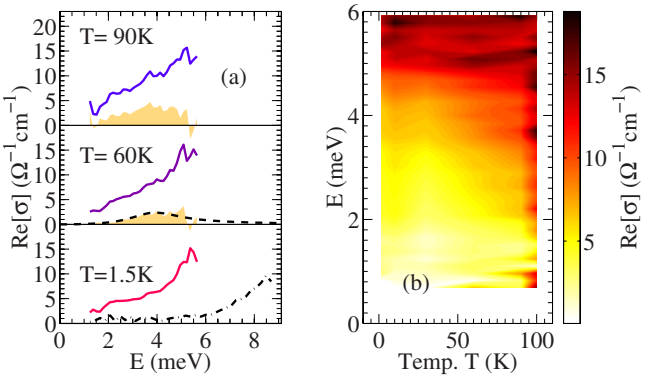

FIG. 4. (Color online) Low-energy conductivity of incommensurate LSNO ($x=0.275$). (a) At 1.5 K, Re$[\sigma]$ for $x=0.275$ (lower solid line) is substantially larger than for $x=0.33$ (dash-dotted line). The charge density wave response Re$[\sigma_{CDW}]$ (dashed line) again agrees with the experimental Re$[\Delta\sigma]$ (shaded area), but at a lower pinning energy $\hbar\omega_0=3.9$ meV. The temperature dependence of Re$[\sigma]$ is shown in (b).

oscillator strength of the collective mode (with peak conductivity $\sim 5\ \Omega^{-1}\,\text{cm}^{-1}$) is much smaller than that of single-particle excitations ($\sim 600\ \Omega^{-1}\,\text{cm}^{-1}$),[14] which indicates that the effective mass of the collective mode is large.[18]

Although the resonant lineshape in Eq. (1) is also characteristic of a number of quasiparticles, including surface plasmons,[23] excitons,[28] and TO phonons,[27] these can be ruled out for the following reasons. Interactions with surface plasmons (ω_0=plasmon frequency) can be eliminated as the conductivity measurement was of a bulk sample, with no near-field coupling. While transitions between localized charge-transfer exciton states are present in LSNO,[29] resonances lie at ~ 4 eV, far above the meV energy range. The observed resonant line shape at 5.4 meV cannot result from the lowest TO-phonon mode at 19 meV,[14] since Im$[\sigma]$ [Fig. 2(b)], which is strongly sensitive to the phonon line shape, is essentially independent of T.

Intriguingly, the oscillator strength of the collective mode rapidly increases close to T_{co}, as indicated for Re$[\Delta\sigma]$ at $T=190$ K in Fig. 2(a) and by the increase in Re$[\Delta\sigma]$ with T in Fig. 3(b). In Ref. 30, the change in $n(T)/m^*(T)$ for a charge density wave was calculated using a mean field approach including impurity scattering, and was found to rapidly increase toward the Peierls transition temperature. This change may be interpreted as a decrease in the effective mass $m^*=\hbar^2[d^2E(k)/dk^2]^{-1}$: As the Peierls gap closes, the curvature of the electronic bands $E(k)$ is enhanced.

A useful way to evaluate charge transport mechanisms is to compare the temperature dependence of the conductivity with the thermally activated form

$$\Delta\sigma(T) = Ae^{-E_a/k_BT}. \tag{2}$$

In Fig. 3(b), the experimental temperature dependence of Re$[\Delta\sigma]$ at a photon energy of 5 meV is shown as an Arrhenius plot (crosses). Two linear regions can be seen, indicating that two different activation energies are present. The experimental data can be modeled using the sum of two terms of the form of Eq. (2), with fit parameters $E_a=15$ meV, $A=6\ \Omega^{-1}\,\text{cm}^{-1}$ and $E_a=140$ meV, $A=15\,000\ \Omega^{-1}\,\text{cm}^{-1}$ (solid line). The high activation energy mode is consistent with the presence of a midinfrared optical gap,[14–16] and dominates at high temperatures. Therefore, we conclude that the collective mode that we observe near 5 meV for $70<T<180$ K is superimposed on the low-energy tail of the higher-energy midinfrared optical gap, which obscures the CDW-like response at higher temperatures.

The analysis presented earlier has provided evidence for the collective motion of charge stripes [Fig. 2, Eq. (1)]. To investigate this further, we have measured the conductivity of LSNO at incommensurate doping levels. In Fig. 4(a), Re$[\sigma]$ is shown for $x=0.275$ (solid lines). At $T=1.5$ K, the conductivity again exhibits a non-Drude frequency dependence, and is substantially higher than that for $x=0.333$ (dash-dotted line) over the measured range 1–6 meV. The enhanced conductivity of incommensurate LSNO correlates with the disruption of charge stripe ordering seen in neutron scattering measurements[9,10] and schematically illustrated in Fig. 1. No pseudogap in the conductivity is observed, indicating that a dynamic response of the charge stripes exists even at $T=1.5$ K. At enhanced lattice temperatures, the real part of the conductivity again increases, as illustrated in Fig. 4(b) and by the points in Fig. 3(b). Calculating $\Delta\sigma$ for $x=0.275$ allowed the thermally activated response to be identified, in the same way as for $x=0.333$. As for commensurate doping, a CDW response [Eq. (1)] gives good agreement with the experimental $\Delta\sigma$ at $T=60$ K, indicated by the dashed line and shaded area in Fig. 4(a). However, in this case, the pinning energy $\hbar\omega_0=3.9$ meV is lower than that found for $x=0.333$. This result can be explained by the presence at incommensurate doping levels of kinks and discommensurations, which disrupt charge stripe ordering (Fig. 1), and would be expected to reduce the pinning energy. The other fit parameters were $\sigma_0=2.3\ \Omega^{-1}\,\text{cm}^{-1}$ and $\Gamma=4\times 10^{12}\ \text{s}^{-1}$. The oscillator strength of the thermally activated

response for $x=0.275$ at $T=60$ K is comparable to that of $x=0.333$ at $T=130$ K, a finding consistent with the lower pinning energy. In addition, the activation energy for incommensurate LSNO is reduced: The solid blue line in Fig. 3 was obtained using Eq. (2) with $E_a=4.8$ meV.

Whereas the dynamics of spins in stripe-ordered nickelates has been studied in detail,[7] the present results represent the first clear evidence for collective charge dynamics. Here, we have reported that charge stripes in commensurate LSNO ($x=0.333$) have a thermally activated collective mode at 5.4 meV, while at an incommensurate doping level ($x=0.275$) the mode is at 3.9 meV. Correspondingly, the conductivity at incommensurate doping is higher, and the activation energy of the conductivity lower, than in the commensurate case. Whereas many CDWs are purely one dimensional, in this system the charge stripes have a lateral extent. Hence, the collective mode reported here may be longitudinal, as in a classical CDW, or transverse as suggested by recent theoretical work.[31]

The possibility of experimentally studying collective stripe modes, as demonstrated here using terahertz time-domain spectroscopy, provides an incentive for the further development of theories of charge stripe dynamics.[3,31,32] Since an understanding of dynamical stripes may elucidate the physics of high-T_c superconductors, an extension of these measurements to doped cuprates will also be of great interest.

The authors would like to acknowledge financial support from the EPSRC (UK).

*Present address: ETH Zurich, Institute of Quantum Electronics, Wolfgang-Pauli-Strasse 16 HPT-H7, 8093 Zurich, Switzerland. james.lloyd-hughes@phys.ethz.ch

†m.johnston@physics.ox.ac.uk

[1] V. J. Emery, S. A. Kivelson, and J. M. Tranquada, Proc. Natl. Acad. Sci. U.S.A. **96**, 8814 (1999).

[2] S. A. Kivelson, I. P. Bindloss, E. Fradkin, V. Oganesyan, J. M. Tranquada, A. Kapitulnik, and C. Howald, Rev. Mod. Phys. **75**, 1201 (2003).

[3] C. M. Smith, Y. A. Dimashko, N. Hasselmann, and A. O. Caldeira, Phys. Rev. B **58**, 453 (1998).

[4] S. A. Kivelson, E. Fradkin, and V. J. Emery, Nature (London) **393**, 550 (1998).

[5] J. M. Tranquada, B. J. Sternlieb, J. D. Axe, Y. Nakamura, and S. Uchida, Nature (London) **375**, 561 (1995).

[6] J. M. Tranquada, H. Woo, T. G. Perring, H. Goka, G. D. Gu, G. Xu, M. Fujita, and K. Yamada, Nature (London) **429**, 534 (2004).

[7] J. M. Tranquada, P. Wochner, and D. J. Buttrey, Phys. Rev. Lett. **79**, 2133 (1997); A. T. Boothroyd, D. Prabhakaran, P. G. Freeman, S. J. S. Lister, M. Enderle, A. Hiess, and J. Kulda, Phys. Rev. B **67**, 100407(R) (2003); P. Bourges, Y. Sidis, M. Braden, K. Nakajima, and J. M. Tranquada, Phys. Rev. Lett. **90**, 147202 (2003); A. T. Boothroyd, P. G. Freeman, D. Prabhakaran, A. Hiess, M. Enderle, J. Kulda, and F. Altorfer, *ibid.* **91**, 257201 (2003).

[8] C. H. Chen, S. W. Cheong, and A. S. Cooper, Phys. Rev. Lett. **71**, 2461 (1993).

[9] S. H. Lee and S. W. Cheong, Phys. Rev. Lett. **79**, 2514 (1997).

[10] J. M. Tranquada, D. J. Buttrey, V. Sachan, and J. E. Lorenzo, Phys. Rev. Lett. **73**, 1003 (1994); V. Sachan, D. J. Buttrey, J. M. Tranquada, J. E. Lorenzo, and G. Shirane, Phys. Rev. B **51**, 12742 (1995); H. Yoshizawa, T. Kakeshita, R. Kajimoto, T. Tanabe, T. Katsufuji, and Y. Tokura, *ibid.* **61**, R854 (2000).

[11] C. H. Du, M. E. Ghazi, Y. Su, I. Pape, P. D. Hatton, S. D. Brown, W. G. Stirling, M. J. Cooper, and S. W. Cheong, Phys. Rev. Lett. **84**, 3911 (2000).

[12] R. Klingeler, B. Buchner, S. W. Cheong, and M. Hucker, Phys. Rev. B **72**, 104424 (2005).

[13] P. G. Freeman, A. T. Boothroyd, D. Prabhakaran, and J. Lorenzana, Phys. Rev. B **73**, 014434 (2006).

[14] T. Katsufuji, T. Tanabe, T. Ishikawa, Y. Fukuda, T. Arima, and Y. Tokura, Phys. Rev. B **54**, R14230 (1996).

[15] P. Calvani, A. Paolone, P. Dore, S. Lupi, P. Maselli, P. G. Medaglia, and S. W. Cheong, Phys. Rev. B **54**, R9592 (1996).

[16] J. H. Jung, D. W. Kim, T. W. Noh, H. C. Kim, H. C. Ri, S. J. Levett, M. R. Lees, D. M. Paul, and G. Balakrishnan, Phys. Rev. B **64**, 165106 (2001).

[17] C. C. Homes, J. M. Tranquada, Q. Li, A. R. Moodenbaugh, and D. J. Buttrey, Phys. Rev. B **67**, 184516 (2003).

[18] G. Grüner, Rev. Mod. Phys. **60**, 1129 (1988).

[19] N. Kida and M. Tonouchi, Phys. Rev. B **66**, 024401 (2002).

[20] M. Fujita, H. Goka, K. Yamada, and M. Matsuda, Phys. Rev. Lett. **88**, 167008 (2002).

[21] D. Grischkowsky, J. Opt. Soc. Am. B **7**, 2006 (1990).

[22] C. Schmuttenmaer, Chem. Rev. (Washington, D.C.) **104**, 1759 (2004).

[23] P. Parkinson, J. Lloyd-Hughes, Q. Gao, H. H. Tan, C. Jagadish, M. B. Johnston, and L. M. Herz, Nano Lett. **7**, 2162 (2007).

[24] J. Li, Y. Zhu, J. M. Tranquada, K. Yamada, and D. J. Buttrey, Phys. Rev. B **67**, 012404 (2003).

[25] M. E. Ghazi, P. D. Spencer, S. B. Wilkins, P. D. Hatton, D. Mannix, D. Prabhakaran, A. T. Boothroyd, and S. W. Cheong, Phys. Rev. B **70**, 144507 (2004).

[26] D. Prabhakaran, P. Isla, and A. T. Boothroyd, J. Cryst. Growth **237**, 815 (2002).

[27] M. B. Johnston, L. M. Herz, A. L. T. Khan, A. Köhler, A. G. Davies, and E. H. Linfield, Chem. Phys. Lett. **377**, 256 (2003).

[28] R. A. Kaindl, M. A. Carnahan, D. Hagele, R. Lovenich, and D. S. Chemla, Nature (London) **423**, 734 (2003).

[29] E. Collart, A. Shukla, J. P. Rueff, P. Leininger, H. Ishii, I. Jarrige, Y. Q. Cai, S. W. Cheong, and G. Dhalenne, Phys. Rev. Lett. **96**, 157004 (2006).

[30] T. W. Kim, D. Reagor, G. Grüner, K. Maki, and A. Virosztek, Phys. Rev. B **40**, 5372 (1989).

[31] L. Benfatto and C. M. Smith, Phys. Rev. B **68**, 184513 (2003).

[32] E. Kaneshita, M. Ichioka, and K. Machida, J. Phys. Soc. Jpn. **70**, 866 (2001).